Supporting information

Deconstructing excitation transitions in Dy^{3+}-doped $CaWO_4$ to develop a new ratiometric luminescent thermometry for achieving ultra-high sensing sensitivity

ianrui Liu,[a,b] Baosheng Cao,[b,*] Miao Gao,[b] Lulu Qiu,[b] Yujie Weng,[b] Yangyang He,[b] Xiaoguang Han,[a,*] Bin Dong[b]

[1] Department of Materials Science and Engineering, Dalian Maritime University, Dalian 116026, P. R. China

[2] Key Laboratory of Photosensitive Material and Device of Liaoning Province, Key Laboratory of New Energy and Rare Earth Resource Utilization of State Ethnic Affairs Commission & School of Physics and Materials Engineering, Dalian Minzu University, Dalian 116600, P. R. China

*Corresponding Authors. E-mail: bscao@dlnu.edu.cn (B. Cao), xghan@dlmu.edu.cn (X. Han)

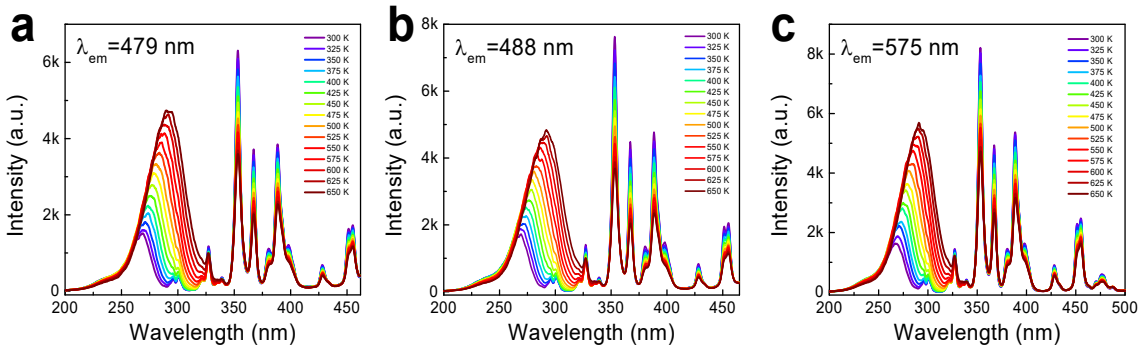

Figure S1. PLE spectra of $CaWO_4$:1Dy phosphors at the temperature range of 300 ~ 650 K by monitoring emissions at λ_{em} = 479 nm (a), 488 nm (b), and 575 nm (c).

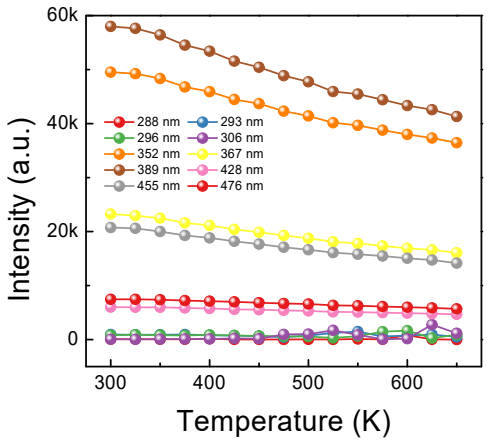

Figure S2. PLE intensities of various Dy^{3+} excitation branches as a function of temperature for $CaWO_4$:1Dy phosphors by monitoring emissions at λ_{em} = 575 nm.

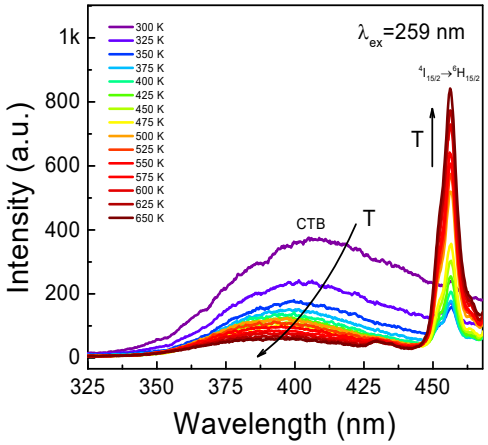

Figure S3. PL spectra of $CaWO_4$:1Dy phosphors at the temperature range of 300 ~ 650 K for λ_{ex} = 259 nm.

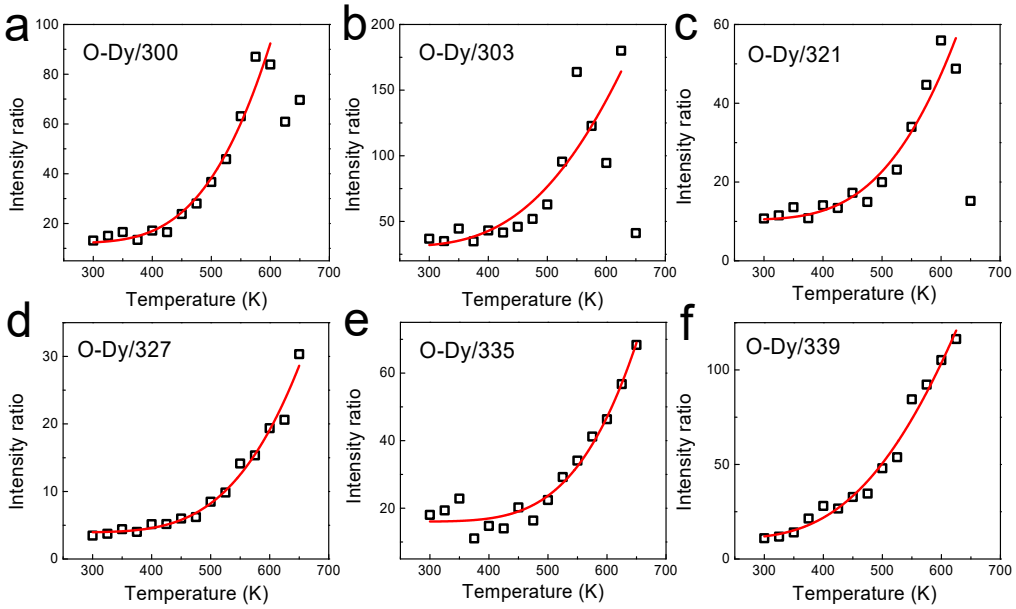

Figure S4. Fit of the temperature-dependent PLE intensity ratio of O-Dy to various Dy^{3+} excitation branches by Eq. (1).

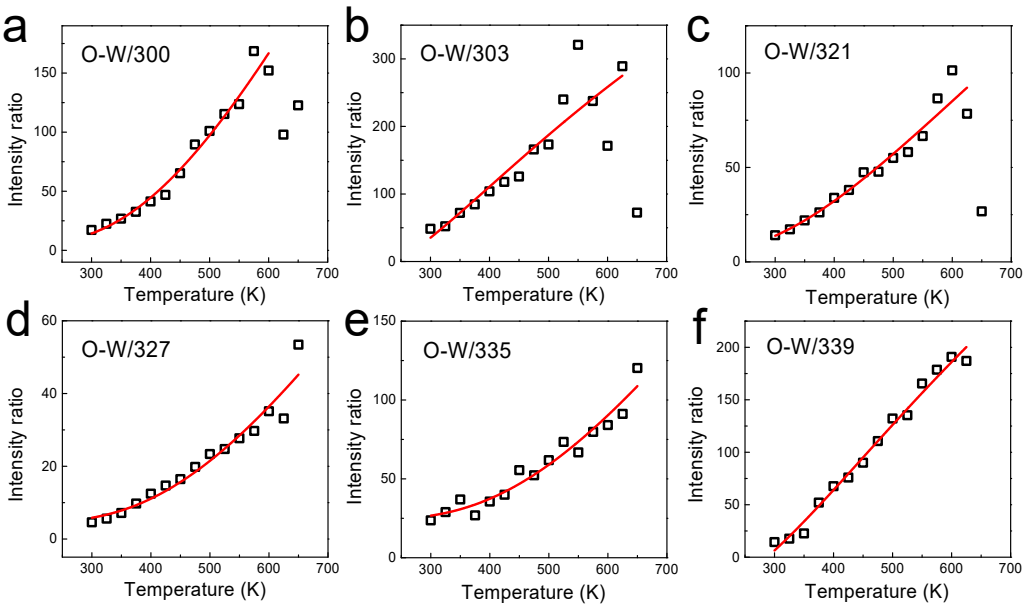

Figure S5. Fit of the temperature-dependent PLE intensity ratio of O-W to various Dy^{3+} excitation branches by Eq. (1).

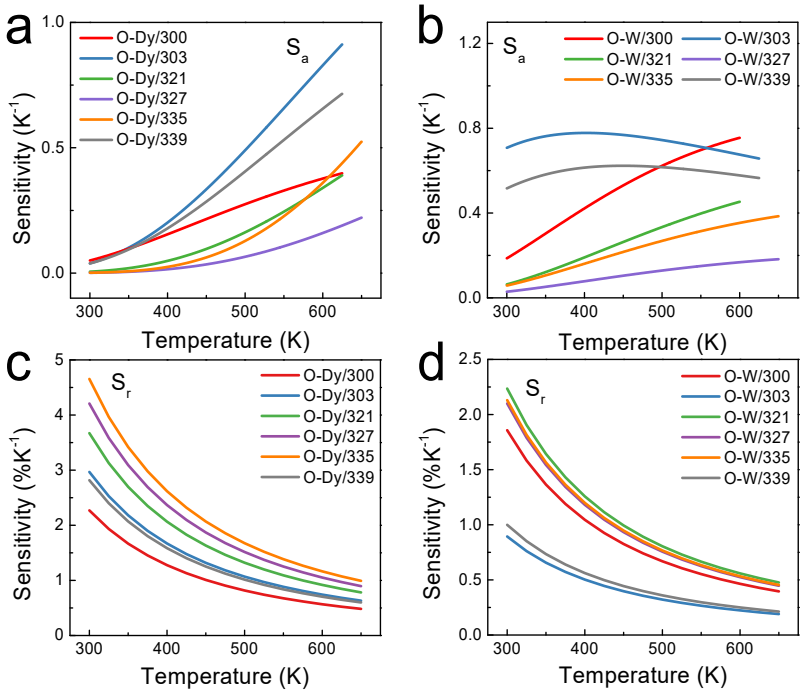

Figure S6. Absolute sensitivity S_a (a,b) and relative sensitivity S_r (c,d) as a function of temperature for the EIR schemes of O-Dy and O-W to various Dy^{3+} excitation branches.

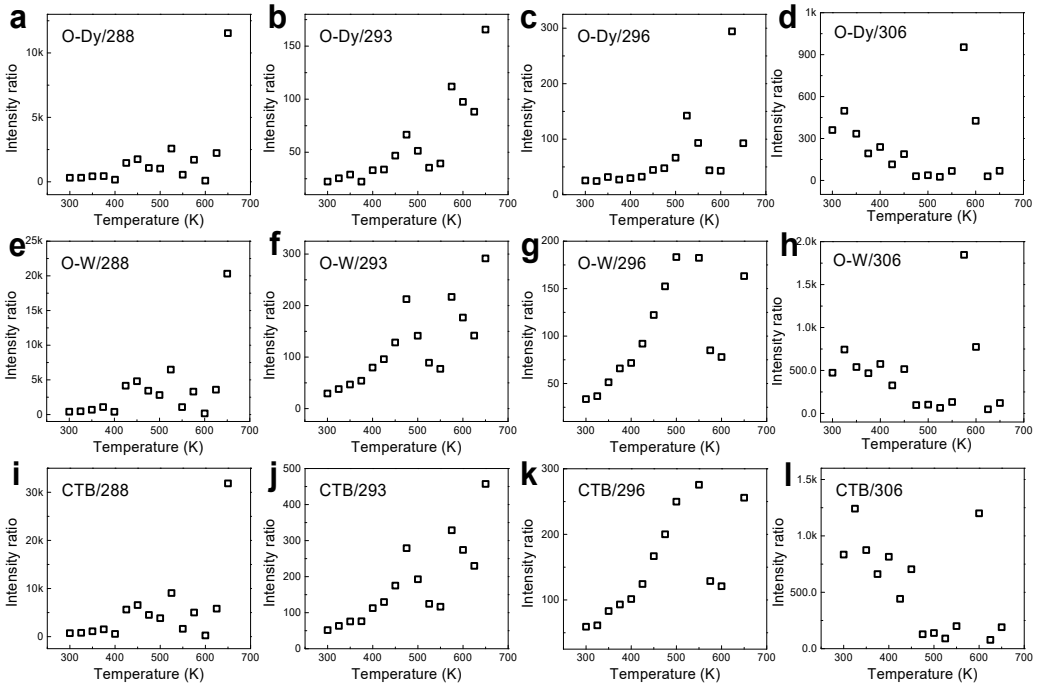

Figure S7. PLE intensity ratio of O-Dy/O-W/CTB to various Dy^{3+} excitation branches as a function of temperature for $CaWO_4$:1Dy phosphors.

Table S1. Experimental PLE and PL transitions in $CaWO_4$:Dy phosphors.

		Transition		Wavelength (nm)	Energy (cm^{-1})	Transition		Wavelength (nm)	Energy (cm^{-1})
PLE	CTB		O-Dy	250	40000				
			O-W	267	37453				
	Dy^{3+}	$^6H_{13/2}$ →	$^4F_{3/2}$	288	34722		$(^4G,^2F)_{7/2}$	321	31153
			$^4P_{1/2}$	293	34130		$^6P_{3/2}$	327	30581
			$(^4L,^4K)_{13/2}$	296	33784		$^4I_{9/2}$	335	29851
			$^4G_{9/2}$	300	33333		$(^4F,^4D)_{5/2}$	339	29499
			$(^4G,^4P)_{5/2}$	303	33003	$^6H_{15/2}$ →	$^6P_{7/2}$	352	28409
			$(^4G,^4H)_{7/2}$	306	32680		$^6P_{5/2}$	367	27248
							$^4I_{13/2},^4F_{7/2}$	389	25707
							$^4G_{11/2}$	428	23364
							$^4I_{15/2}$	455	21978
							$^4F_{9/2}$	476	21008
PL	CTB			410	24390				
	Dy^{3+}	$^4F_{9/2}$ →	$^6H_{15/2}$	482	20747				
			$^6H_{13/2}$	575	17391				
			$^6H_{11/2}$	663	15083				

Table S2. Fitting parameters of $EIR = a \cdot exp\left(-\frac{b}{T}\right) + c$ for the various EIR schemes in $CaWO_4$:Dy phosphors.

EIR scheme		EIR range	Fitting parameter		
			a	b	c
O-Dy/	300	13.1~69.7	1998.11	2042.09	7.17
	303	36.8~180	9572.44	2670.45	30.7
	321	10.8~55.9	9114.04	3303.78	10.4
	327	3.47~30.3	8369.77	3786.94	3.94
	335	18.0~68.3	2534.87	4188.56	16.04
	339	10.9~116.3	6364.64	2534.87	10.6
	352	0.42~2.21	113.69	2622.95	0.38
	367	0.90~5.00	269.19	2646.62	0.81
	389	0.36~1.95	103.02	2638.39	0.32
	428	3.48~17.19	933.85	2666.36	3.15
	455	1.01~5.68	313.03	2664.81	0.91
	476	2.80~14.12	816.34	2705.41	2.55
O-W/	300	17.23~168.53	2636.79	1671.67	4.21
	303	48.32~289.21	1155.59	804.21	-44.02
	321	14.11~101.40	2318.75	2011.93	14.62
	327	4.56~83.75	746.21	1890.04	4.46
	335	23.69~120.30	1620.95	1917.46	23.96
	339	14.38~190.83	1034.95	899.27	-45.24
	352	0.55~3.88	17.84	941.89	-0.3
	367	1.18~8.81	43.65	1004.29	-0.53
	389	0.47~3.43	16.42	977.58	-0.23
	428	4.57~30.22	135.94	935.68	-2.05
	455	1.32~9.99	49.99	1016.02	-0.56
	476	3.68~24.87	117.5	981.7	-1.22
CTB/	300	30.35~255.57	8867.92	2176.43	22.09
	303	85.11~362.53	9344.32	2014.47	76.61
	321	24.86~157.34	2822.27	1943.52	22.06
	327	8.03~83.75	3454.23	2594.56	10.09
	335	41.73~188.56	10211.85	2819.27	44.85
	339	25.32~303.27	3008.21	1386.49	-9.48
	352	0.98~6.09	57.58	1505.53	0.56
	367	2.08~13.81	141.45	1557.71	1.23
	389	0.83~5.37	53.16	1535.8	0.49
	428	8.05~47.38	449.24	1517.6	4.98
	455	2.33~15.67	163.03	1571.49	1.40
	476	6.49~38.99	394.9	1561.93	4.23